**Electronic supplementary materials** *Mendeleev Commun.*, 2022, **32**, 609–611

# Synthesis and antiviral properties of tricyclic amides derived from α-humulene and β-caryophyllene

**Olga I. Yarovaya, Kseniya S. Kovaleva, Sophia S. Borisevich, Tatyana V. Rybalova, Yuriy V. Gatilov, Ekaterina O. Sinegubova, Alexandrina S. Volobueva, Vladimir V. Zarubaev and Nariman F. Salakhutdinov**

## 1. Chemistry

### 1.1. General Information

Reagents and solvents were purchased from commercial suppliers and used as received. Dry solvents were obtained according to standard procedures. Reactions monitoring, the content of the compounds in fractions during chromatography and the purity of the target compounds were determined using 7890A gas chromatograph (Agilent Tech., USA) with an Agilent 5975C quadrupole mass spectrometer as detecto HP-5 capillary column, He as carrier gas (flow rate 2 ml/min, flow division 99:1). $^{1}$H and $^{13}$C NMR spectra were recorded on Bruker spectrometers, including an AV-300 instrument at 300.13 MHz ($^{1}$H) and 75.47 MHz ($^{13}$C), an AV-400 instrument at 400.13 MHz ($^{1}$H) and 100.61 MHz ($^{13}$C), and a DRX-500 instr ument at 500.13 MHz ($^{1}$H) and 125.76 MHz ($^{13}$C) in $CDCl_3$; chemical shifts δ were report ed in ppm relative to residual $CHCl_3$ [d($CHCl_3$) 7.24, d($CDCl_3$) 76.90 ppm], *J* in Hz. We used caryophyllene $[\alpha]_{580}^{20}$ - 13.8 ($CHCl_3$, c 4.3). Compound **4** was previously synthesized and described [S1].

### 1.2. Transformations of humulene in the system of acetonitrile-sulfuric acid.

***N*-(2,2,4,8-Tetramethyldecahydro-4,8-methanoazulen-9-yl)acetamide 3.**

To a solution of humulene (0.5 g) in acetonitrile (10 ml), sulfuric acid (0.2 ml) was added. The mixture was stirred for 20 min, then neutralized with saturated $Na_2CO_3$ solution. White needle-like crystals of amide **3** (mp 201-203 $^{o}$C) precipitated from the organic layer on standing. The product was filtered, washed with hexane to afford 0.37 g (57%) of compound **3**.

### 1.3. NMR spectra

**Table S1.** Correlation of the signals in the NMR spectra in amide **3**

| C-position | $^{13}$C NMR (125 MHz) | $^{1}$H NMR (500 MHz) |
|---|---|---|
| 1,5 | 41.4 | - |
| 2,4 | 32.8 | 1.16 (4H, o) |
| 3 | 18.4 | 1.57 (1H, m)<br>1.43 (1H, m) |
| 6,10 | 47.5 | 2.16 (2H, m) |
| 7,9 | 43.1 | 1.33 (2H, m)<br>1.16 (2H, o) |
| 8 | 39.3 | - |
| 11 | 56.7 | 3.75 (1H, d, J=10.2) |
| 12 | 170.1 | - |
| 13 | 23.8 | 2.02 (3H, s) |
| 14,15 | 20.6 | 0.73 (6H, s) |
| 16 | 28.4 | 1.05 (3H, s) |
| 17 | 25.5 | 0.87 (3H, s) |
| NH | - | 5.35 (1H, d, J=10.2) |

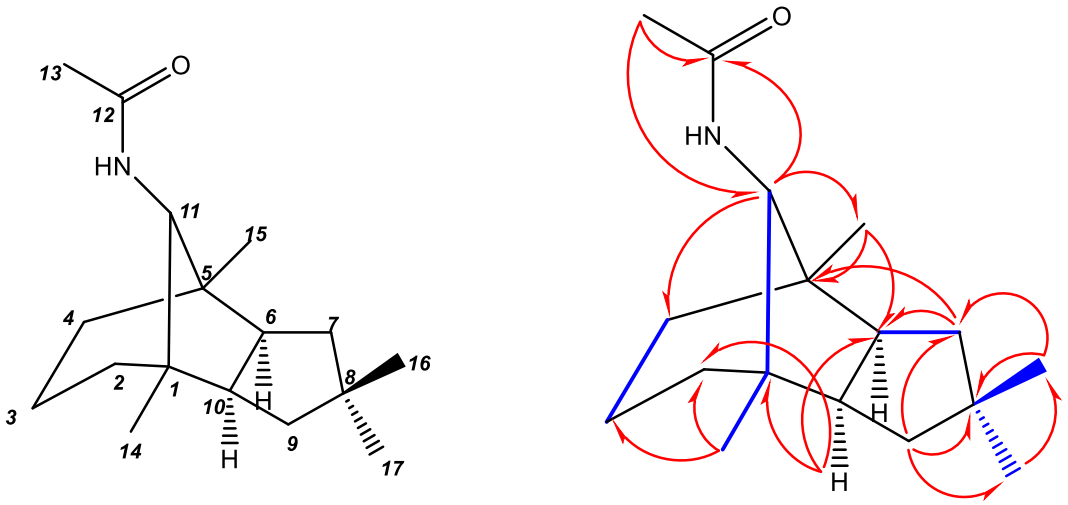


**Figure S1.** Key HMBC (red arrows) and 1H-1H COSY ( blue bold) correlation in amid **3**.

**$^{1}$H, 400 MHz, $CDCl_3$**

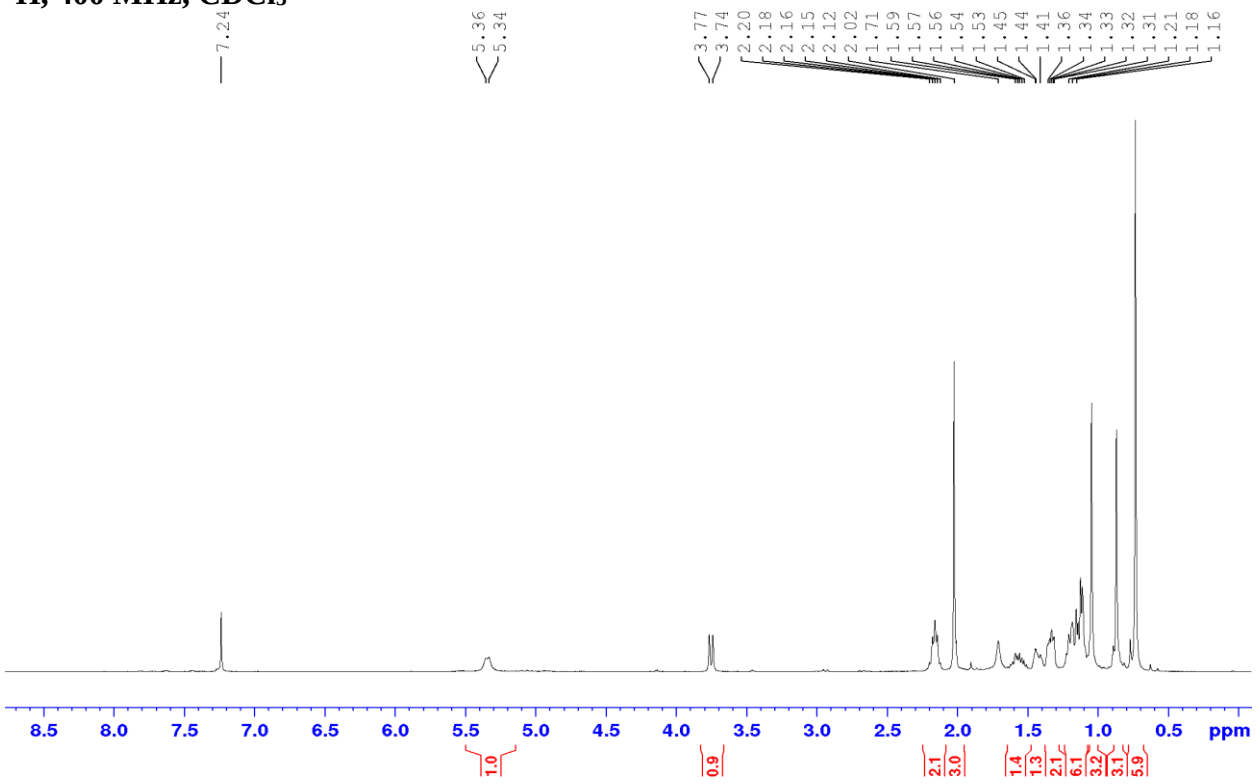


**$^{13}$C, 100 MHz, JMOD**

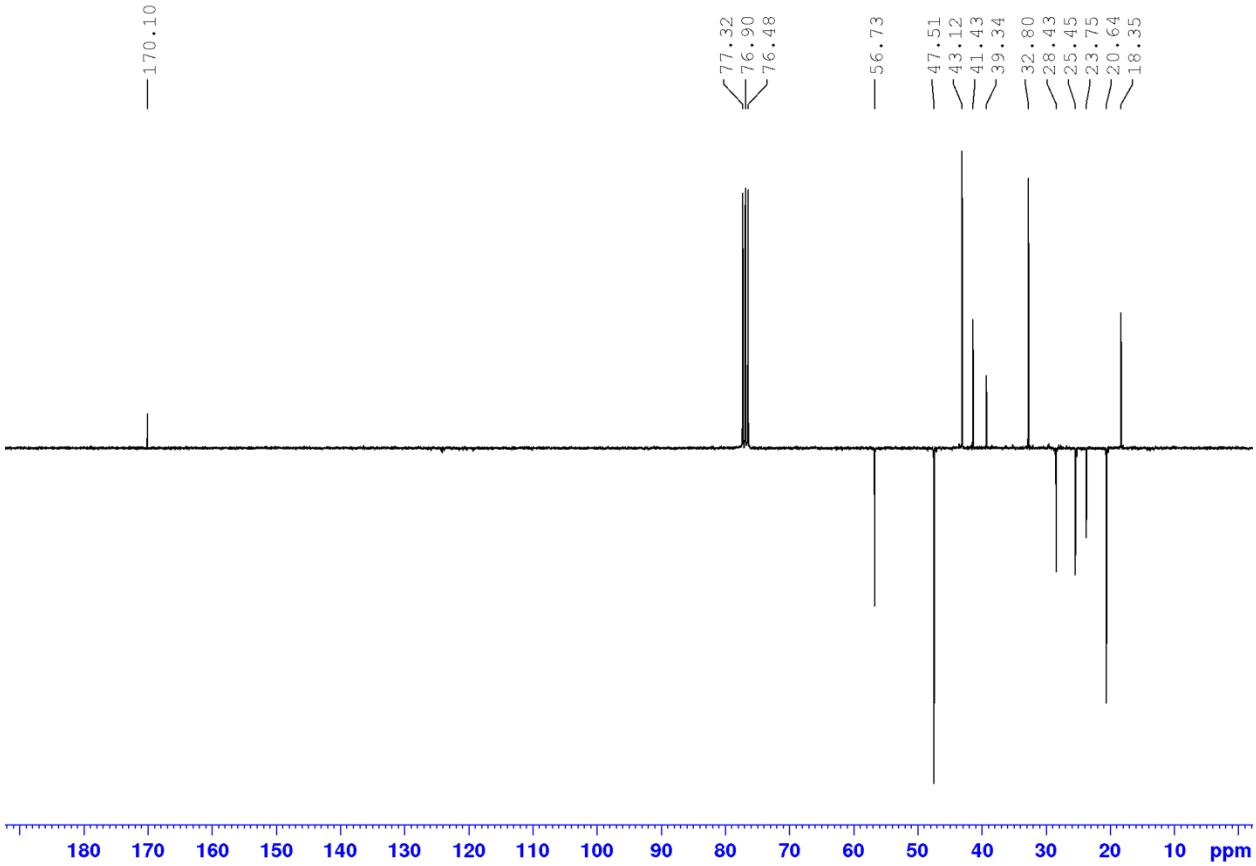

**$^{13}$C, 100 MHz, BB**

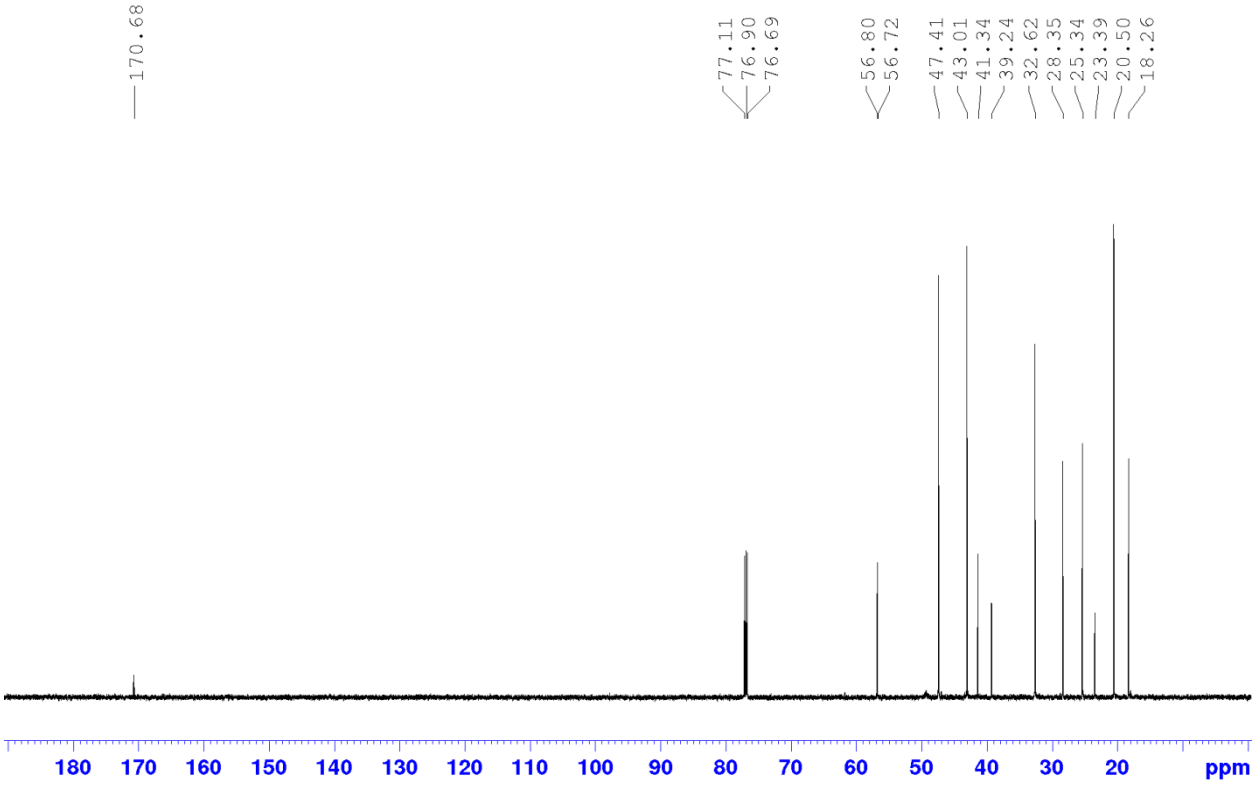


**$^{1}$H-$^{1}$H, NOESY**

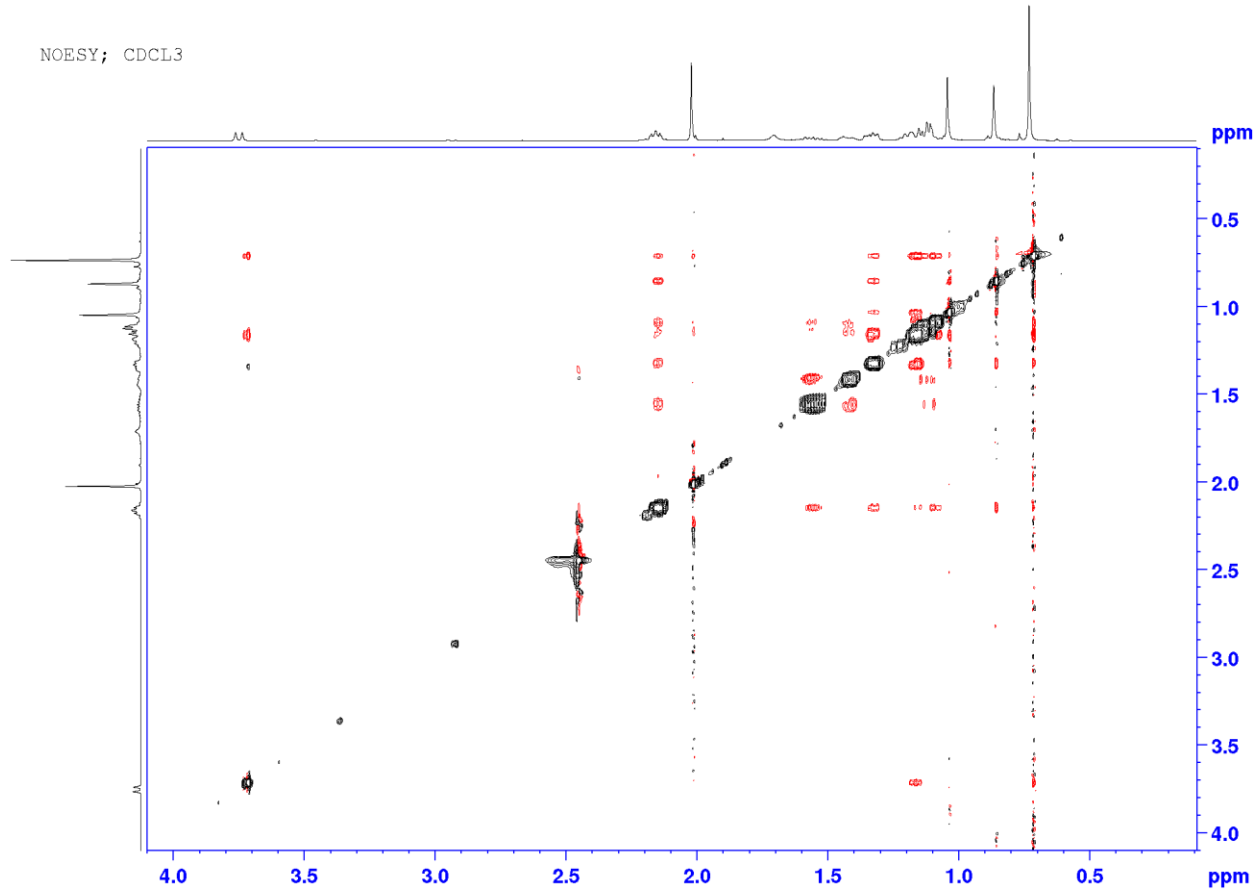

**$^{1}$H-$^{1}$H, COSY**

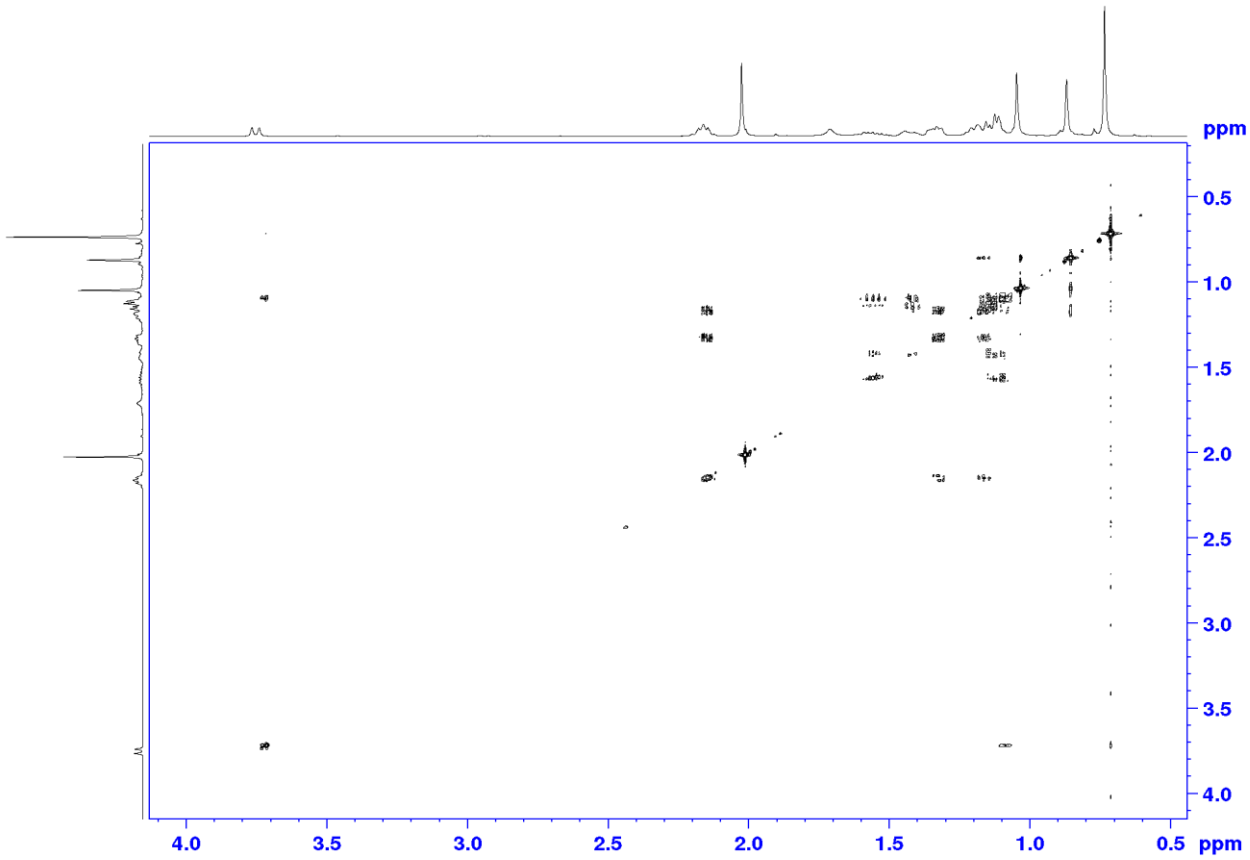


**$^{1}$H-$^{13}$C, HSQC**

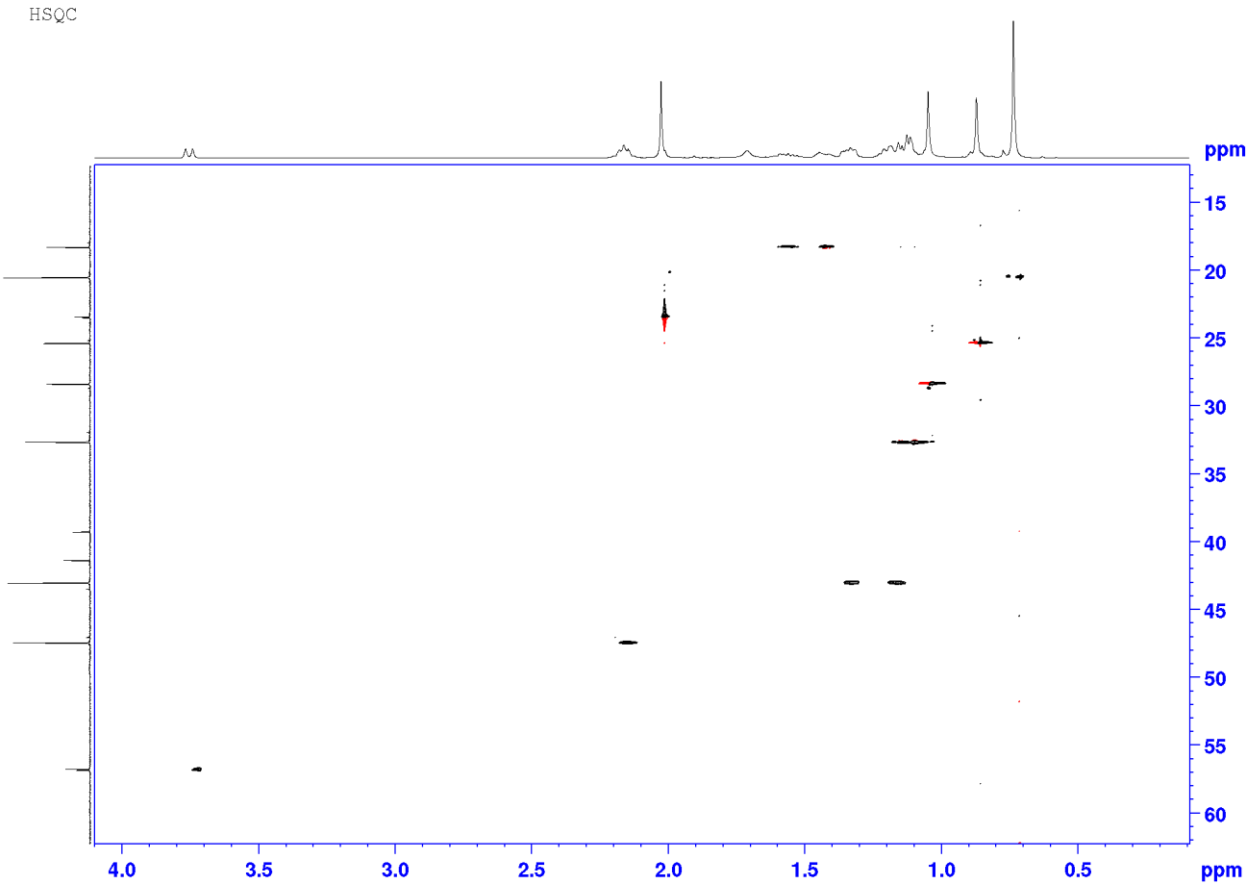

**$^{1}H$-$^{13}C$, HMBC**

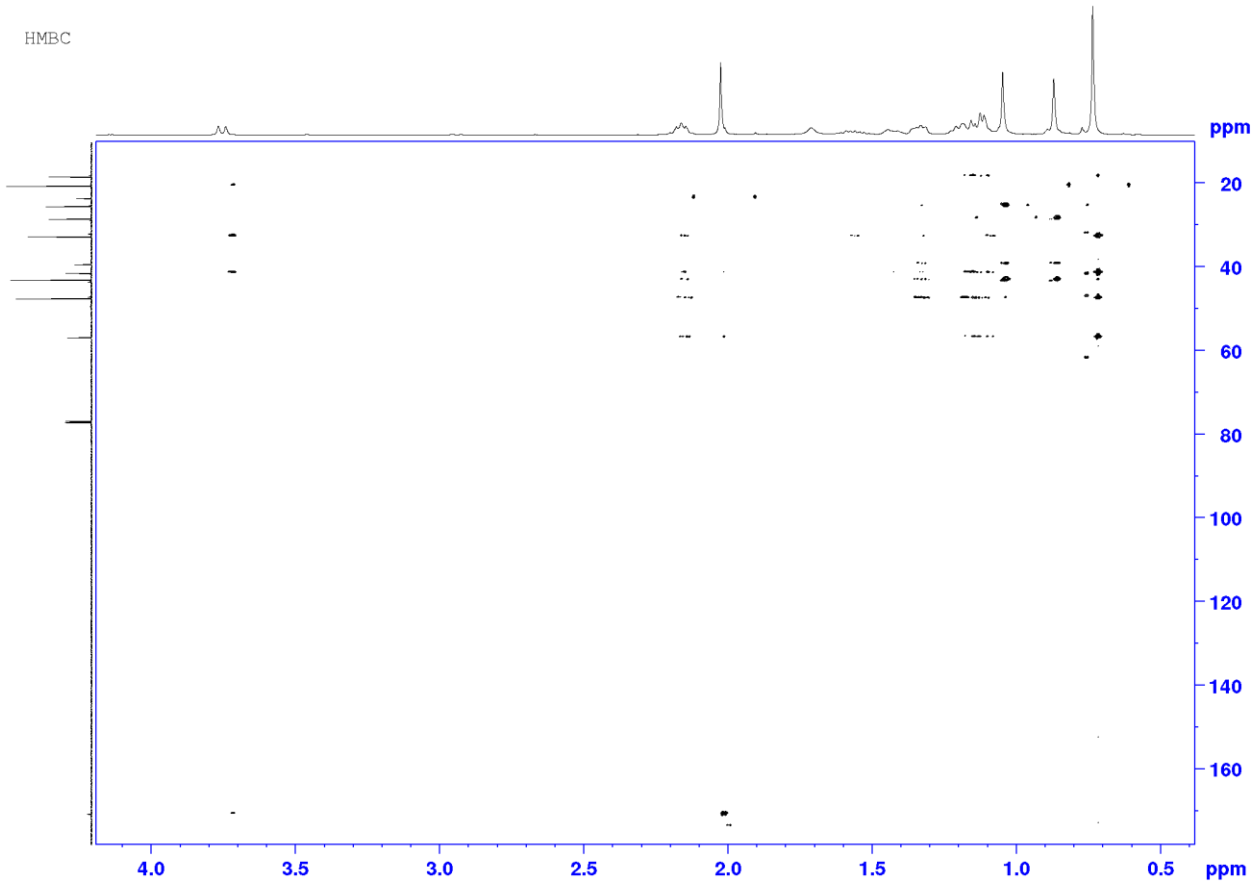
HMBC
ppm
20
40
60
80
100
120
140
160
4.0
3.5
3.0
2.5
2.0
1.5
1.0
0.5
ppm

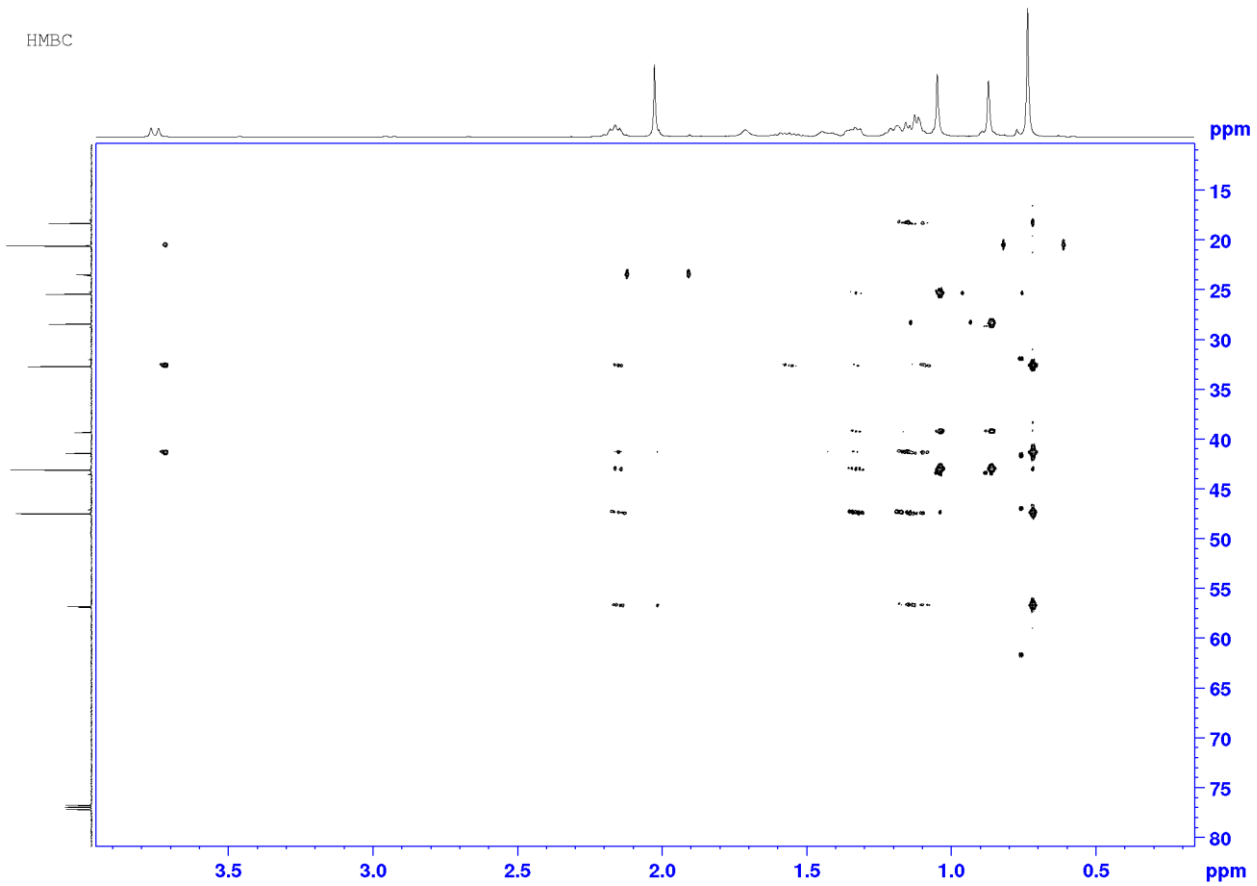
HMBC
ppm
15
20
25
30
35
40
45
50
55
60
65
70
75
80
3.5
3.0
2.5
2.0
1.5
1.0
0.5
ppm

### 1.4. X-ray analysis

The structure of compounds **3** and **4** was determined by the single crystal X-ray analysis. The analysis of the geometry and the intermolecular interactions was performed using PLATON program [S2]. The bond lengths in the molecule are close to the averaged statistical values [S3].

Crystallographic data for the structure have been deposited at the Cambridge Crystallographic Data Centre as supplementary publication no. CCDC2152454-2152455. Copy of the data can be obtained free of charge, on application to CCDC, 12 Union Road, Cambridge CB21EZ, UK (fax: +44 122 3336033 or e-mail: deposit@ccdc.cam.ac.uk; internet: www.ccdc.cam.ac.uk).

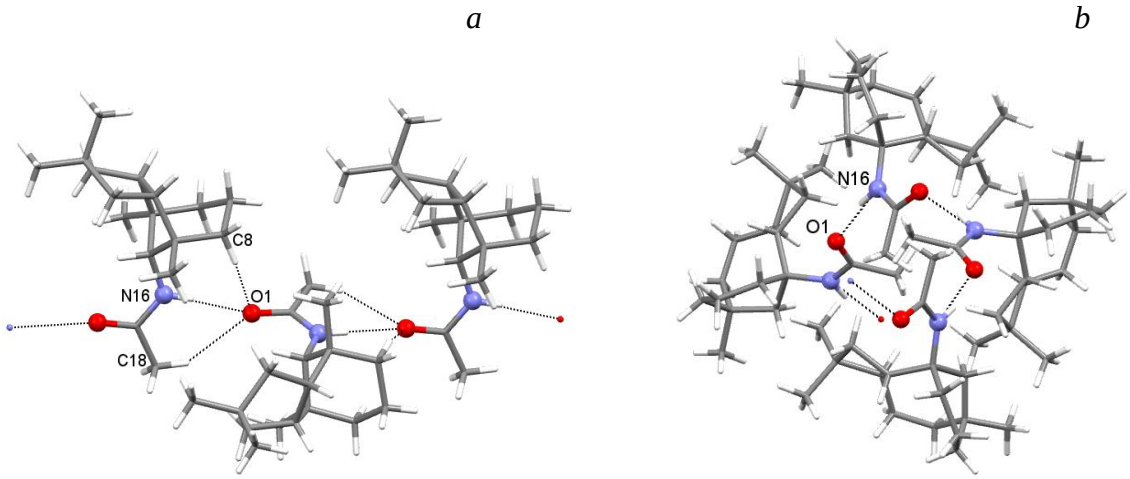


**Figure S2** The hydrogen-bonded chains in crystals of (*a*) compund **3** and (*b*) compound **4** directed along the axis *c*.

## 2. Biological testing

### 2.1. Cytotoxicity determination.

The microtetrazolium test (MTT) was used to study the cytotoxicity of the compounds [S4]. Briefly, series of three-fold dilutions of each compound in MEM were prepared. MDCK cells were incubated for 48 h at 36ºC in 5% $CO_2$ in the presence of the dissolved substances. The cells were washed twice with phosphate-buffered saline (PBS), and a solution of 3-(4,5-dimethylthiazol-2-yl)-2,5-diphenyltetrazolium bromide (ICN Biochemicals Inc. Aurora, Ohio) (0.5 μg/ml) in PBS was added to the wells. After 1 h incubation, the wells were washed and the formazan residue was dissolved in DMSO (0.1 ml per well). The optical density of cells was then measured on a Victor 2 1440 multifunctional reader (Perkin Elmer, Finland) at wavelength of 535 nm and plotted against the concentration of compounds. Each concentration was tested in three parallels. The 50% cytotoxic concentration ($CC_{50}$) of each compound was calculated from the data obtained.

### 2.2. Anti-viral assay

The compounds in appropriate concentrations (300 - 3 μg/ml) were dissolved in DMSO (0.1 ml) and final solutions were prepared by adding MEM with 1 μg/ml trypsin. Compounds were incubated with MDCK cells at 36 °C for 1 h. Each concentration of the compounds was tested in triplicate. The cell culture was then infected with influenza virus A/Puerto Rico/8/34 (H1N1) (moi 0.01) for 24 h at 36 °C in the presence of 5% $CO_2$. A virus titer in the supernatant was determined by hemagglutination test after cultivating of the virus in MDCK cells for 48 h at 36 °C in the presence of 5% $CO_2$. For calculations, virus titer was expressed as per cent of the titer in control wells without compounds. The 50% inhibiting concentrations ($IC_{50}$) and the selectivity index (SI, the ratio of $CC_{50}$ to $IC_{50}$) were calculated for each compound from the data obtained.

## 3. Computation details

### 3.1. Protein and ligand preparation

The crystallographic structure of influenza virus hemagglutinin (HA) (PDB code 1RU7 [S5] was downloaded from the Protein Data Bank database [S6]. Model protein structures were prepared for calculation: hydrogen atoms were added and minimized; missing amino acid side chains were added; bond multiplicities were restored; solvent molecules were removed; and the entire structure was restrained and optimized in the OPLS3e force field [S7] at 5.0 pH value.
The geometric parameters of potential ligands (amide **3** and **4**) were also optimized.

### 3.2. Active site analysis

According to previous publications [S8-S10], the CPH site was considered a potential binding site. The site is located at the site of proteolysis and is saturated with hydrophobic amino acids such as valine, leucine, isoleucine, tyrosine, alanine, and phenylalanine. Valine ($Val_2615$) is considered a key amino acid.HA sequencing of Camphecene- and Ginsamide-resistant strains of influenza virus showed a mutation $Val_2615Leu$. The pharmacophore profile of Camphecene, Ginsamide, and amides is similar: there is a large hydrophobic part and a small hydrophilic part containing nitrogen and oxygen atoms.For this reason, we assume that amides can bind at the site.

### 3.3. Molecular docking procedure

Molecular docking procedures and dynamics were performed using Schrodinger Suite (Release 2021-2) software [Schrödinger Release 2021-2: . New York, NY : Schrödinger, LLC, 2021]. Lead-compounds were docked using the forced ligand positioning protocol (IFD) with the following conditions: flexible protein and ligand; grid matrix size of 15 Å; and amino acids (within a radius of 5 Å from the ligand) restrained and optimized, considering the influence of the ligand. However binding energies ($\Delta G_{bind}$) ligand-protein complexes were estimated using variable-dielectric generalized Born model, which incorporates residue-dependent effects. The solvent is water.

## References


S1 O. I. Yarovaya, D. V. Korchagina, T. V. Rybalova, Y. V. Gatilov, M. P. Polovinka and V. A. Barkhash, *Russ. J. Org. Chem.*, 2004, **40**, 1593–1598.

S2 A. L. Spek, *J. Appl. Crystallogr.*, 2003, **36**, 7–13.

S3 F. H. Allen, O. Kennard, D. G. Watson, L. Brammer, A. G. Orpen and R. Taylor, *J. Chem. Soc. Perkin Trans. 2*, 1987, S1.

S4 T. Mosmann, *J. Immunol. Methods*, 1983, **65**, 55–63.

S5 S. J. Gamblin, L. F. Haire, R. J. Russell, D. J. Stevens, B. Xiao, Y. Ha, N. Vasisht, D. A. Steinhauer, R. S. Daniels, A. Elliot, D. C. Wiley and J. J. Skehel, *Science*, 2004, **303**, 1838–42.

S6 H. M. Berman, J. Westbrook, Z. Feng, G. Gilliland, T. N. Bhat, H. Weissig, I. N. Shindyalov and P. E. Bourne, *The Protein Data Bank*, 2000, vol. 28.

S7 D. Shivakumar, E. Harder, W. Damm, R. A. Friesner and W. Sherman, *J. Chem. Theory Comput.*, 2012, **8**, 2553–2558.

S8 A. S. Volobueva, O. I. Yarovaya, M. V. Kireeva, S. S. Borisevich, K. S. Kovaleva, I. Y. Mainagashev, Y. V. Gatilov, M. G. Ilyina, V. V. Zarubaev and N. F. Salakhutdinov, *Molecules*, 2021, **26**, 6794.

S9 V. V Zarubaev, E. A. Pushkina, S. S. Borisevich, A. V Galochkina, A. V Garshinina, A. A. Shtro, A. A. Egorova, A. S. Sokolova, S. L. Khursan, O. I. Yarovaya and N. F. Salakhutdinov, *Virology*, 2018, **524**, 69–77.

S10 S. S. Borisevich, M. A. Gureev, O. I. Yarovaya, V. V. Zarubaev, G. A. Kostin, Y. B. Porozov and N. F. Salakhutdinov, *J. Biomol. Struct. Dyn.*, 2021, doi.org/10.1080/07391102.2020.1871414.